Proceedings of the 4th International Conference on Software Engineering and Machine Learning
DOI: 10.54254/2755-2721/2026.32158

Factor-Graph-Based Multi-Source Integrated Navigation for UAVs

Qingyang An

School of Mechatronic Engineering, Changchun University of Science and Technology, Changchun, China
an1563247798@163.com

Abstract. Reliable navigation under GNSS degradation requires exploiting complementary sensors and estimation methods that can tolerate nonlinearity and outliers. This paper presents a multi-source integrated navigation approach for unmanned aerial vehicles (UAVs) that combines an inertial measurement unit (IMU), GNSS, a ground-based laser ranging-and-angle sensor, and a ground-based RF radar. A practical calibration and alignment pipeline is first established, including IMU intrinsic calibration (misalignment, scale factors, and biases), GNSS lever-arm compensation, and weighted least-squares calibration for range/angle channels of the laser sensor and radar. On this basis, a sliding-window factor-graph optimization framework is constructed with IMU preintegration as the time backbone, while GNSS, laser, and radar measurements are introduced as factors. Marginalization is applied to bound the problem size, and residual-based down-weighting is used to suppress gross errors. Simulation results on a maneuvering UAV trajectory demonstrate clear accuracy gains over an extended Kalman filter (EKF): the mean position error decreases from about 2.16–2.20 m to 0.69–0.79 m, and the mean velocity error decreases from about 0.24–0.28 m/s to 0.10–0.11 m/s. These results indicate that factor-graph smoothing can provide more accurate and stable navigation estimates for multi-rate heterogeneous sensing.

Keywords: UAV navigation, Multi-sensor fusion, Factor graph optimization, Sensor calibration, Marginalization

1. Introduction

Unmanned aerial vehicle (UAV) navigation in complex environments requires robust state estimation under nonlinearity, multi-rate sensing, and occasional measurement outliers [1]. Classical filter-based fusion, such as the extended Kalman filter (EKF), relies on local linearization and a Markov assumption, which may lead to degraded performance when the sensing model is highly nonlinear or when the noise characteristics deviate from ideal Gaussian assumptions [2]. To improve accuracy and robustness, this work focuses on a factor-graph optimization (FGO) approach for multi-source integrated navigation, supported by a practical sensor calibration and alignment pipeline [3].

DOI: 10.54254/2755-2721/2026.32158

2. Methodology

2.1. Sensor calibration and alignment

Before multi-source fusion, sensor intrinsic parameters and inter-sensor geometry must be calibrated to ensure that heterogeneous measurements are expressed in a consistent reference frame. The calibration procedures include IMU intrinsic calibration, GNSS lever-arm compensation, laser ranging-and-angle calibration, RF radar calibration, and multi-sensor initial alignment [4].

Low-cost inertial sensors are subject to cross-axis misalignment, scale-factor errors, and biases, which directly affect attitude, velocity, and position estimates. Assuming negligible installation misalignment between the body frame and the IMU sensor frame, the calibrated accelerometer and gyroscope outputs are modelled as:

$$a'_{IMU} = T_a K_a a_{IMU} - b_a \tag{1}$$

$$\omega'_{IMU} = T_\omega K_\omega \omega_{IMU} - b_\omega \tag{2}$$

where T_a and T_ω represent misalignment matrices, K_a and K_ω are diagonal scale-factor matrices, and b_a and b_ω denote biases. A least-squares formulation is used to estimate calibration parameters based on measurements collected at six static orientations (six faces).

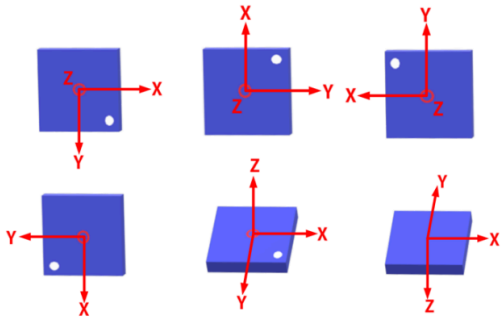

Figure 1. IMU placement orientations for six-face calibration

Table 1. Calibrated accelerometer intrinsic parameters

S_{ayx}	S_{azx}	S_{azy}	K_{ax}	K_{ay}	K_{az}	b_{ax}	b_{ay}	b_{az}
0.02	0.01	0.01	0.99	1.01	0.98	0.51	0.65	0.82

Table 2. Calibrated gyroscope intrinsic parameters

$S_{\omega yx}$	$S_{\omega zx}$	$S_{\omega zy}$	$K_{\omega x}$	$K_{\omega y}$	$K_{\omega z}$	$b_{\omega x}$	$b_{\omega y}$	$b_{\omega z}$
0.02	0.01	0.02	0.99	1.00	0.98	-1.51	1.52	1.01

In practice, the GNSS antenna cannot coincide with the IMU reference point. A fixed lever arm between the GNSS antenna phase center and the IMU geometric center introduces a systematic position/velocity offset in the navigation solution. Let δl_b denote the lever-arm vector expressed in the body frame. The position of the GNSS antenna in the navigation frame can be expressed by adding the rotated lever arm to the IMU-centered position estimate:

$$P_{GNSS} = P_{IMU} + C_b^n \delta l_b \tag{3}$$

DOI: 10.54254/2755-2721/2026.32158

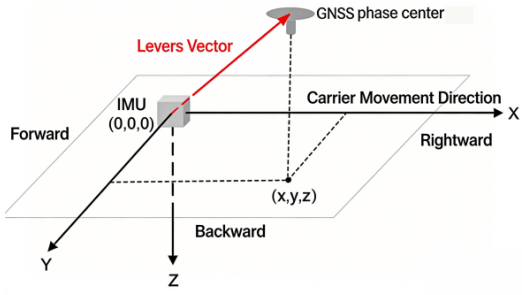

Figure 2. GNSS lever-arm geometry between GNSS antenna and IMU reference point

A slant laser triangulation ranging module is used together with a two-axis gimbal encoder that provides azimuth and elevation angles. The ranging model relates the target distance S to the image-plane displacement S′. In engineering implementation, the sensor output is typically a pixel coordinate u, which is mapped to S′ via a linear model, followed by a first-order correction for residual systematic errors:

$$S' = k_u(u - u_0) \tag{4}$$

$$S_c = k_s S + b_s \tag{5}$$

Azimuth and elevation angles are calibrated with scale and bias terms. Weighted least squares is used to estimate calibration parameters from N reference samples, while robust loss functions can be adopted to mitigate outliers caused by occlusion, strong reflections, or tracking failures. Range-dependent measurement uncertainty is characterized via error propagation, noting that triangulation ranging typically degrades at long distances.

The ground RF radar provides slant range ρ as well as azimuth and elevation angles. To enable fusion in an ENU navigation frame, radar extrinsics and channel-wise systematic errors are calibrated using reference positions. Residuals of (ρ, α, β) are minimized using weighted least squares, and robust reweighting is applied to reduce the influence of multipath and false alarms. The measurement covariance used in fusion is constructed from residual statistics, potentially as a range-dependent diagonal model:

$$R_R = diga(\sigma_\rho^2(\rho), \sigma_\alpha^2(\rho), \sigma_\beta^2(\rho)) \tag{6}$$

Multi-source information fusion can be described by an observation model in which measurements are generated as a (generally nonlinear) mapping of the state plus noise:

$$Z = h(x) + w \tag{7}$$

Depending on implementation constraints, fusion can be organized in centralized, distributed, or hybrid architectures. Centralized fusion directly processes raw measurements from all sensors, whereas distributed fusion performs local estimation at multiple nodes and then fuses local estimates using weighting factors. Hybrid fusion combines both strategies and trades computation and communication resources for improved robustness [5].

DOI: 10.54254/2755-2721/2026.32158

2.2. Multi-source fusion modelling

Prepare your paper using clear and well written English. Poorly written English may obscure the scientific merit of your paper. Avoid using first person point of view (such as "I", "we") wherever possible. Please carefully proofread your manuscript in terms of spelling and grammar before submission.

2.3. Integrated navigation coupling modes

For GNSS/INS integrated navigation, three coupling modes are commonly discussed: loosely coupled, tightly coupled, and deeply coupled. Loosely coupled fusion uses GNSS position/velocity solutions as measurements, tightly coupled fusion directly integrates pseudorange and Doppler-type observables, and deep coupling further increases the receiver–INS interaction at the signal-processing level. Considering engineering complexity, the proposed multi-source system follows an indirect fusion strategy and leverages external sensors (laser and radar) to support navigation when GNSS is unavailable.

2.4. Optimal state estimation and factor graph optimization

Sliding-window smoothing requires maintaining a finite set of states. To keep the computation bounded during long operations, old states are marginalized out and their information is converted into a prior factor that constrains the remaining window.

The multi-sensor estimation problem is formulated as a nonlinear least-squares optimization. Common solvers include Gauss–Newton and Levenberg–Marquardt, where the latter introduces a trust-region strategy to improve numerical stability when the Hessian matrix is ill-conditioned.

A factor graph represents the estimation problem as a bipartite graph with state nodes and factor nodes. Each factor encodes a likelihood term derived from a sensor measurement or a prior constraint. IMU measurements, due to their high sampling rate, define the time backbone of the sliding window, while measurements from other sensors are associated with the nearest IMU epoch or inserted as dedicated nodes when necessary.

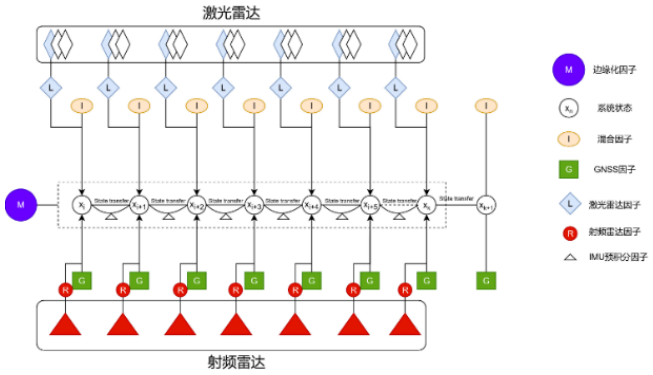

Figure 3. Conceptual factor graph with state nodes and measurement factors

DOI: 10.54254/2755-2721/2026.32158

3. Factor-graph-based multi-source fusion algorithms

3.1. INS/GNSS factor graph

For the INS/GNSS case, the state at epoch k is defined as position $p_{ins,k}^T$, attitude quaternion $q_{ins,k}^T$, velocity $v_{ins,k}^T$, accelerometer bias $b_{a,k}^T$,k, and gyroscope bias $b_{g,k}^T$:

$$x_k = [p_{ins,k}^T, q_{ins,k}^T, v_{ins,k}^T, b_{a,k}^T, b_{g,k}^T]^T \tag{8}$$

The objective function includes GNSS position residual factors, IMU preintegration residual factors, and a marginalization prior:

$$min_x F(X) = \sum_{i\in[o,m]} \|r_{GNSS}(X, Z_{GNSS}^i)\|_{GNSS}^2 + \sum_{k\in[1,n]} \|r_{pre}(X, Z_{pre}^k)\|_{pre}^2 + \|\delta M(X)\|^2 \tag{9}$$

Nonlinear optimization is implemented using the Ceres Solver with a Levenberg–Marquardt strategy. For post-processing, forward and backward solutions can be fused by weighted averaging. When GNSS is healthy, equal weights are used; during GNSS outages, the weights are designed to decrease with outage duration to reduce the influence of diverging inertial-only propagation.

3.2. INS/GNSS/laser fusion

Laser ranging-and-angle measurements are introduced as additional factors to support localization during GNSS outages. A keyframe-based sliding window is adopted, where the window size is determined by the number of keyframes rather than a fixed number of time epochs. Two-stage optimization is used: after an initial optimization, residuals are evaluated to down-weight GNSS gross errors and remove laser factors that exhibit large residuals, improving robustness to outliers.

3.3. INS/GNSS/laser/RF radar fusion

RF radar factors are further added to the factor graph to improve robustness in adverse conditions. When a radar measurement arrives, its timestamp is compared with existing nodes; if the time difference is below a threshold, the measurement is associated with the nearest node using the IMU-propagated pose; otherwise, a new node is created at the radar epoch and inserted into the optimization window.

4. Simulation experiments

4.1. Simulation setup

A maneuvering UAV trajectory is simulated to validate the proposed methods. The flight contains acceleration, turns, deceleration, and descent. The main sensor parameters used in simulation are summarized in Table 3.

DOI: 10.54254/2755-2721/2026.32158

Table 3. Sensor parameters used in simulation

Sensor Type	Parameters	numerical value
SINS	gyro constant bias(°/h)	5
	gyro angle random walk (°/$\sqrt{h}$)	0.05
	accelerometer constant bias(μg)	50
	accelerometer random noise(m/s/$\sqrt{h}$)	5
	update period	0.01s
GNSS	positioning error	[3m,3m,5m]
	velocity error	0.1m/s
	update period	1s
Laser	range accuracy	0.5m
	update period	0.2s
RF radar	slant range accuracy	1m
	update period	0.5s

4.2. Results and analysis

The factor-graph approach is compared with an EKF baseline. Figures 4 and 5 illustrate the position and velocity error time histories, and Table 4 summarizes maximum and mean errors. The factor graph achieves lower peak and average errors across all components.

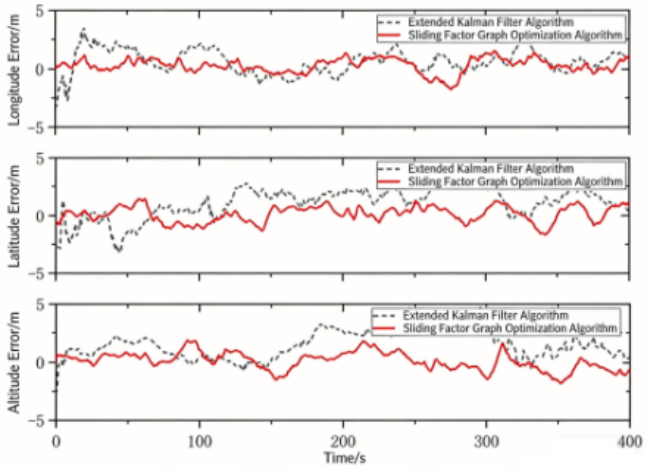

Figure 4. Position error comparison between EKF and factor graph optimization

DOI: 10.54254/2755-2721/2026.32158

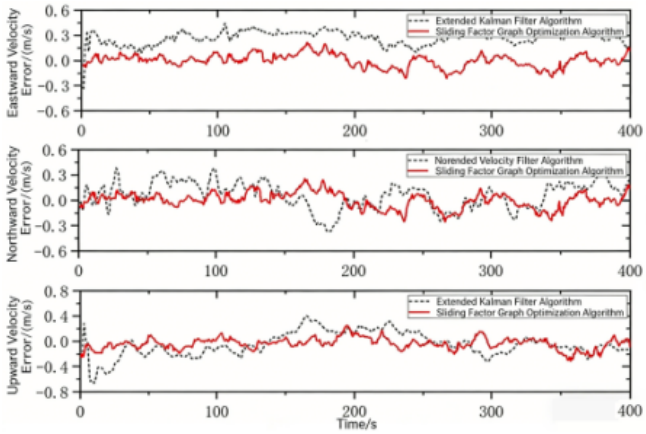

Figure 5. Velocity error comparison between EKF and factor graph optimization

Table 4. Simulation error statistics for EKF and factor graph optimization

Algorithm Type	Statistics Type	Longitude error /m	Latitude error /m	Height error /m	Eastward Velocity Error/(m/s)	Northward Velocity Error/(m/s)	Celestial Velocity Error/(m/s)
EKF	MAX	4.2951	4.3285	4.0561	0.4837	0.5117	0.7012
	MEAN	2.1606	2.1854	2.2010	0.2390	0.2485	0.2816
Factor graph	MAX	1.5692	1.7398	1.8945	0.3217	0.3336	0.3019
	MEAN	0.6948	0.7353	0.7867	0.1128	0.1095	0.1016

5. Conclusion

The simulation indicates that sliding-window factor-graph smoothing can outperform EKF filtering for nonlinear multi-source navigation. The improvement is attributed to jointly optimizing multiple epochs, explicitly modelling heterogeneous measurement factors, and incorporating marginalization priors rather than relying solely on a first-order Markov recursion.

A factor-graph optimization framework with IMU preintegration, sliding-window marginalization, and robust reweighting was formulated for multi-rate heterogeneous fusion. Simulation results demonstrate that factor-graph optimization reduces both mean position and velocity errors compared with an EKF baseline, supporting its use for accurate and robust navigation in complex sensing conditions.

References

[1] Xin S, Wang X, Zhang J, et al. A Comparative Study of Factor Graph Optimization- Based and Extended Kalman Filter-Based PPP-B2b/INS Integrated Navigation [J]. Remote Sensing, 2023, 15(21): 5144.

[2] Dellaert F, Kaess M. Factor graphs for robot perception [J]. Foundations and Trends® in Robotics, 2017, 6(1-2): 1-139.

[3] Tang H, Zhang T, Niu X et al. 2022. Impact of the Earth rotation compensation on MEMS-IMU printegration of factor graph optimization [J]. IEEE Sens. J., 22(17): 17194-17204.

[4] Chang L, Niu X, Liu T, et al. GNSS/INS/LiDAR-SLAM integrated navigation system based on graph optimization [J]. Remote Sensing, 2019, 11(9): 1009.

[5] Wen Z, Guo X, Zheng Z, et al. TL-GILNS: A trajectory-layer-enhanced GNSS/INS/LiDAR integrated approach towards reliable positioning and accurate accuracy quantification [J]. IEEE Internet of Things Journal, 2024.